

# Dynamic monitoring of blood oxygen saturation *in vivo* using double-ring photoacoustic sensor

Guangzhi Yin, Da Xing,<sup>a)</sup> and Sihua Yang

MOE Key Laboratory of Laser Life Science and Institute of Laser Life Science, College of Biophotonics, South China Normal University, Guangzhou 510631, China

(Received 2 March 2009; accepted 5 June 2009; published online 13 July 2009)

Photoacoustic (PA) can distinguish oxygenated main chromophores which are hemoglobin (HbO<sub>2</sub>) and deoxygenated hemoglobin (Hb) in blood by the optical absorption at multiple optical wavelengths. In this study, a noninvasive PA system with a double-ring sensor was used for fixed-point measurement of hemoglobin oxygen saturation (SO<sub>2</sub>) continually. The double-ring sensor is an ultrasonic Fresnel zone plate ultrasonic transducer. It has two-zone negative zone plate piezoelectric material pattern with good focusing effect for fixed-point detection of SO<sub>2</sub>. Three specific optical absorbed wavelengths (760, 805, and 850 nm) of HbO<sub>2</sub> and Hb were employed sequentially to obtain PA signals and calculate the SO<sub>2</sub> at each blood oxygen level. The capability and accuracy of the system were tested by phantom samples and *in vitro* blood samples, and the results of the PA detection were in excellent agreement with the data of the control group by the blood-gas analyzer. In *in vivo* studies, the SO<sub>2</sub> of the artery and the vein in a rabbit ear were noninvasively detected. Furthermore, changes in the SO<sub>2</sub> from normal to hypoxia and to hyperoxia due to the changed inhale gas were dynamically recorded by the PA system. The experimental results demonstrate that this PA SO<sub>2</sub> measurement system has the potential for fixed-point detection and dynamic monitoring of blood oxygen saturation. © 2009 American Institute of Physics. [DOI: 10.1063/1.3160297]

## I. INTRODUCTION

Hemoglobin oxygen saturation (SO<sub>2</sub>) is an important physiological index in clinical diagnosis. It reflects the efficiency of cardiopulmonary function since oxygenation level in the circulatory system provides an estimate of tissue oxygenation. Any increase in oxygen consumption of brain or decrease in the oxygen supply can result in changes in jugular venous oxygen saturation. Therefore, in therapy of head injury or digging skull operation, a continuous measurement of jugular venous oxygen saturation is a key index in reflecting the brain's oxygen supply and demand balance.<sup>1-3</sup> Traditional techniques for monitoring of jugular venous oxygen saturation are invasive, maybe take the patients into danger. Therefore, noninvasive and real-time measurement of the blood oxygen saturation is invaluable, especially in extensive surgery.

A current technique for noninvasive monitoring of SO<sub>2</sub> is near-infrared spectroscopy (NIRS).<sup>4,5</sup> NIRS measures SO<sub>2</sub> by the spectroscopic difference between oxygenated hemoglobin and deoxygenated hemoglobin. Pulse oximetry based on NIRS is most widely used on clinic for this purpose. However, pulse oximetry has low spatial resolution for the strong optical scattering in biological tissues, and the detection of oxygen saturation that depends on the pulse can only reflect averaged arterial blood oxygen saturation in certain region at subcutaneous.

Photoacoustic (PA) signal is a result of short duration and localized energy absorption. Such energy deposition can

be supplied by visible, infrared, or microwave radiation. PA waves travel through the target and can be detected by an ultrasonic transducer.<sup>6,7</sup> Therefore, this noninvasive measurement technology combines the excellences of optics and ultrasonics and has high optical contrast and high ultrasonic resolution. It can map the absorbed optical energy deposit in tissues and reflect excellent detailed anatomic blood images of tumor, brain, and other diseases.<sup>8-16</sup>

PA measurement of blood SO<sub>2</sub> relies on the spectroscopic difference of HbO<sub>2</sub> and Hb, which are mainly the absorbing compounds in blood.<sup>17,18</sup> In this study, three optical wavelengths are employed to explode PA signals to accurately quantify these two chromophores. We constructed a PA system with double-ring sensor, which has two-zone negative zone plate piezoelectric material pattern with good focusing effect for fixed-point SO<sub>2</sub> measurement. In contrast with NIRS which measures diffuse light, our system has high spatial resolution and can measure SO<sub>2</sub> at one single vessel. Phantom sample and *in vitro* blood samples were first performed to confirm the accuracy and the stability of this system. The potential application of the system was also demonstrated by successfully monitoring of SO<sub>2</sub> variations in localized vessel *in vivo*.

## II. MATERIALS AND METHODS

### A. Measurement principle

If the laser pulse is sufficiently short, this means that there is insignificant heat relaxation in the irradiated volume during the optical pulse. The relationship of the PA signal  $p(\mathbf{r}, t)$  and the heating source  $H(\mathbf{r}, t)$  can be expressed as

<sup>a)</sup>Author to whom correspondence should be addressed. Electronic mail: xingda@sncnu.edu.cn. Tel.: +86-20-85210089. FAX: +86-20-85216052.

$$\nabla^2 p(\mathbf{r}, t) - \frac{1}{c^2} \frac{\partial^2 p(\mathbf{r}, t)}{\partial t^2} = -\frac{\beta}{C_p} \frac{\partial}{\partial t} H(\mathbf{r}, t). \quad (1)$$

In general, the solution of Eq. (1) in the time domain can be expressed as

$$p(\mathbf{r}, t) = \frac{\beta}{4\pi C_p} \iint \iint \frac{dr'}{|r-r'|} \frac{\partial H(\mathbf{r}', t')}{\partial t'} \bigg|_{t'=t-\frac{|r-r'|}{c}} \quad (2)$$

When the irradiation source is symmetrical, the heating function  $H(\mathbf{r}, t)$  can be written as the product of a spatial absorption function  $A(\mathbf{r})$  and a temporal function  $I(t)$ ,

$$H(\mathbf{r}, t) = A(\mathbf{r})I(t). \quad (3)$$

$I(t)$  can be considered as a Dirac delta function  $\delta(t)$  for a short excited light pulse.  $A(\mathbf{r})$  describes the optical energy deposition which depends on optical absorption coefficient  $\mu^\lambda$  and light density at position  $r$ .

Thus, Eq. (3) can be written as<sup>19,20</sup>

$$p(\mathbf{r}, t) = K\mu^\lambda \varphi(t), \quad (4)$$

where  $K$  is the Grüneisen parameter and  $\varphi(t)$  describes the optical energy deposition at position  $r$ . If the irradiation optical energy density and the structure of the absorbing object are fixed, the optical absorption coefficient  $\mu^\lambda$  of the object is proportional to the amplitude of PA signal  $p(\mathbf{r}, t)$  at position  $r$ .

PA measurement of  $\text{SO}_2$  is similar to NIRS.  $\text{HbO}_2$  and  $\text{Hb}$  are two dominant absorbing compounds in blood at near-infrared band. Because of the spectroscopic difference between hemoglobin and deoxygenated hemoglobin, we can calculate the  $\text{SO}_2$  through Lambert-Beer law.<sup>21,22</sup> It is expressed as

$$\text{SO}_2 = \frac{[\text{HbO}_2]}{[\text{HbO}_2] + [\text{Hb}]} = \begin{cases} \frac{\mu^{\lambda_2} \varepsilon_{\text{Hb}}^{\lambda_1} - \mu^{\lambda_1} \varepsilon_{\text{Hb}}^{\lambda_2}}{\mu^{\lambda_1} \Delta \varepsilon_{\text{Hb}}^{\lambda_2} - \mu^{\lambda_2} \Delta \varepsilon_{\text{Hb}}^{\lambda_1}} \\ \vdots \\ \frac{\mu^{\lambda_{n-1}} \varepsilon_{\text{Hb}}^{\lambda_n} - \mu^{\lambda_n} \varepsilon_{\text{Hb}}^{\lambda_{n-1}}}{\mu^{\lambda_n} \Delta \varepsilon_{\text{Hb}}^{\lambda_{n-1}} - \mu^{\lambda_{n-1}} \Delta \varepsilon_{\text{Hb}}^{\lambda_n}} \end{cases}, \quad (5)$$

where  $\varepsilon_{\text{Hb}}^{\lambda_n}$  is the known molar extinction coefficients ( $\text{cm}^{-1}/\text{M}^{-1}$ ) of  $\text{Hb}$  at wavelength  $\lambda_n$ ,<sup>23,24</sup>  $\mu^{\lambda_n}$  is the absorption coefficient ( $\text{cm}^{-1}$ ) of the whole blood at different wavelength;  $\Delta \varepsilon_{\text{Hb}}^{\lambda} = \varepsilon_{\text{HbO}_2}^{\lambda} - \varepsilon_{\text{Hb}}^{\lambda}$ .

Therefore,  $\text{SO}_2$  can be calculated using the measured PA signal according to Eq. (5). In all of our experiments, PA measurements were conducted at 760, 805, and 850 nm, respectively, for reducing measurement error.

## B. Experimental system

The schematic of the experimental system is given in Fig. 1. An OPO laser (VIBRANT B 532I, OPOTEK, USA) provides irradiation pulses to excite intrinsic PA signals. The laser pulse has a full width at half maximum of 10 ns and a repetition of 10 Hz. The tuning range of the OPO ranged

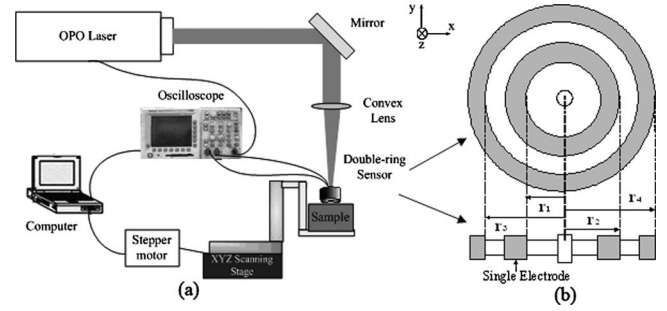


FIG. 1. (a) Experimental setup of PA system based on a double-ring PA sensor for monitoring of  $\text{SO}_2$ . (b) The PA double-ring sensor: cross section along the axis and the piezoelectric (PZT) zone plate pattern of the sensor.

from 680 to 950 nm. A hollow double-ring sensor was employed to collect PA signal. The laser beam was focused by a convex lens through the small hole in the central of double-ring sensor. A digital oscilloscope (TDS3032, Tektronix, USA) received the amplified PA signals from the double-ring sensor at a sampling rate of 500 M samples/s and transferred the digitized signals to a computer for subsequent data processing. At each sampling position, the PA signals were averaged for 16 traces. An X-Y-Z scanning stage is driven by computer-controlled stepper motors.

The double-ring sensor employed in this system had a two-zone negative zone plate piezoelectric material pattern for a good ultrasonic focusing effect. In medium of biological tissues, optical focus is much wider than ultrasonic focus. Therefore, an effective ultrasonic focus transducer conduces to accurate measurement of  $\text{SO}_2$  at fixed position. The lateral resolution of this transducer is approximately  $0.65 \pm 0.015 \text{ mm}$ .<sup>25</sup> It had a central frequency of 2 MHz, a bandwidth of 60% at  $-6 \text{ dB}$ . The acoustic field is focused at a distance of 10 mm on the axis of the double-ring sensor with a length of focus of 3 mm. The radii of zone boundary are  $r_1=2.76 \text{ mm}$ ,  $r_2=3.94 \text{ mm}$ ,  $r_3=4.87 \text{ mm}$ , and  $r_4=5.68 \text{ mm}$ , respectively [Fig. 1(b)]. It operates in reflection mode and it allows scanning in a line or a plane.

## C. Animal mode

A New Zealand rabbit weighting  $\sim 1.5 \text{ kg}$  was employed for the *in vivo* experiment. Before experiment, the fur on the ear of the rabbit was shaved. A dose of 30 mg/kg sodium pentobarbital was administered to anesthetize the rabbit before PA measurement. A custom-built holder for rabbit was used to keep the rabbit moveless. After the rabbit was fixed on the holder, it was transferred to a sample stage. A layer of ultrasonic coupling gel was applied on the surface of the ear of the rabbit to couple ultrasound from the ear of the rabbit to the sensor. The rabbit breathes with a respirator, which delivered inhaled gases with different components in order to change the blood  $\text{SO}_2$  of the rabbit. A pulse oximetry monitored the arterial blood oxygenation and the heart rate of the rabbit during the experiment.

## III. RESULTS

### A. Test on phantom samples

Two experiments were designed to test the sensitivity and the accuracy of this system. In the phantom study, red

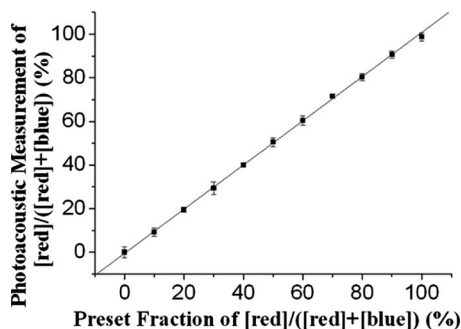


FIG. 2. PA measurement of the fractions of the red ink in the total ink concentration  $[\text{red}]/([\text{red}]+[\text{blue}])$  with a constant interval of 10%.

ink and blue ink were mixed in different concentration ratios to simulate different levels of  $\text{SO}_2$ . The absorption coefficients of red ink at 760, 805, and 850 nm are 19.1, 4.6, and  $1.5 \text{ cm}^{-1}$ , respectively; the absorption coefficients of another blue ink at three wavelengths are 6.1, 4.4, and  $3.4 \text{ cm}^{-1}$ , respectively. The absorption coefficients of ink are measured by spectrophotometer. A transparent silicone tube with an inner diameter of 0.5 mm is filled with ink, which was cycled by a pump and immersed in water. The laser beam at 760, 805, and 850 nm, respectively, irradiated the silicone tube through the ring hole. The fractions of  $[\text{red}]/([\text{red}]+[\text{blue}])$  changed from 0% to 100% with a constant interval of 10%. PA signals from each mixed ink at three wavelengths were collected and calculated by Eq. (1) for the fraction of  $[\text{red}]/([\text{red}]+[\text{blue}])$ . After five tests, the fractions of  $[\text{red}]/([\text{red}]+[\text{blue}])$  were calculated using the PA signals at three wavelengths with less than 1% error compared to the preset values (Fig. 2). The results of phantom samples demonstrate the capability of this PA system to distinguish component in mixed liquid by their different absorption spectra.

### B. *In vitro* study of $\text{SO}_2$

In the *in vitro* study, venous bovine blood was freshly collected and was mixed with anticoagulant before the experiment. The blood samples were saturated with pure oxygen and pure carbon dioxide, respectively, to acquire oxygenated and deoxygenated blood.<sup>24</sup> These two blood samples were mixed at different ratios to gain eight  $\text{SO}_2$  level blood samples,<sup>26</sup> which are from 40.2% to 88.4%. The  $\text{SO}_2$  levels of sample groups were measured by blood-gas analyzer (Stat Profile pHox, Nova Biomedical, USA) before PA detection. Then, each sample was injected into the transparent silicone tube and was promoted smoothly flowed by pump. Figure 3(a) shows the detected signals at three wavelengths at 88.4%  $\text{SO}_2$  level. According to the deduction in Sec. II, multiwavelength PA signals of different  $\text{SO}_2$  levels are proportional to the absorptions of each blood sample, respectively. With detection of PA signal at three wavelengths, the  $\text{SO}_2$  level of each sample was calculated. After a linear analysis with the results of *in vitro* experiment, PA measurements of  $\text{SO}_2$  matched well with the measurements of blood-gas analyzer [Fig. 3(b)]. The above results obtained by this PA system showed that it is reliable and valuable for measuring  $\text{SO}_2$  *in vitro*.

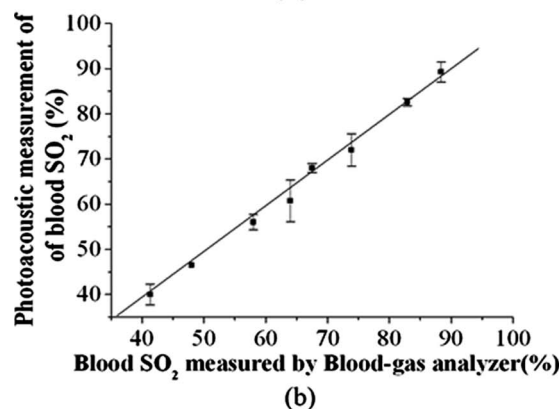
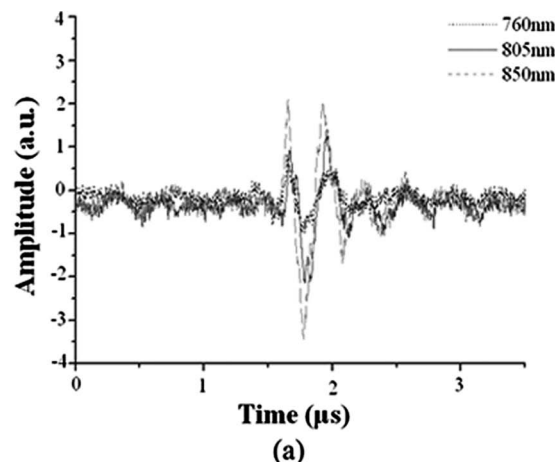


FIG. 3. PA measurement of  $\text{SO}_2$  *in vitro*: (a) the signals of *in vitro* test at 88.4%  $\text{SO}_2$  level; (b) the oxygen saturation of hemoglobin in blood samples *in vitro*.

### C. Monitoring of $\text{SO}_2$ *in vivo*

As shown in Fig. 3(a), the sensor scans along the dotted line with 0.2 mm/step. Two blood vessels across the scan line are detected by PA system at three wavelengths.  $\text{SO}_2$  levels were calculated by PA signals collected at blood vessel positions. As shown in Fig. 3(b), artery and vein can be separated based on the  $\text{SO}_2$  values and change in  $\text{SO}_2$  because the  $\text{SO}_2$  levels of venous and arterial bloods are physiologically distinctive. Compared to the results of pulse oximetry and PA measurement, the arterial  $\text{SO}_2$  value from PA measurement matched well with the measurements of the oximetry.

With the slow decrease in oxygen concentration in the inhaled gas, the blood  $\text{SO}_2$  levels of rabbit were controlled from normal to hypoxia, and the arterial blood oxygenation dropped to  $\sim 80\%$ . Afterward, the inhaled gas was changed

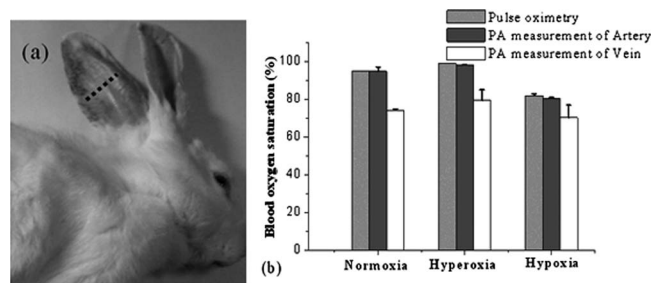


FIG. 4. *In vivo* PA measurements of  $\text{SO}_2$ . (a) Photograph of the rabbit ear with a scanning area. (b)  $\text{SO}_2$  levels of rabbit in normoxia, hyperoxia, and hypoxia were measured by pulse oximetry and PA system, respectively.

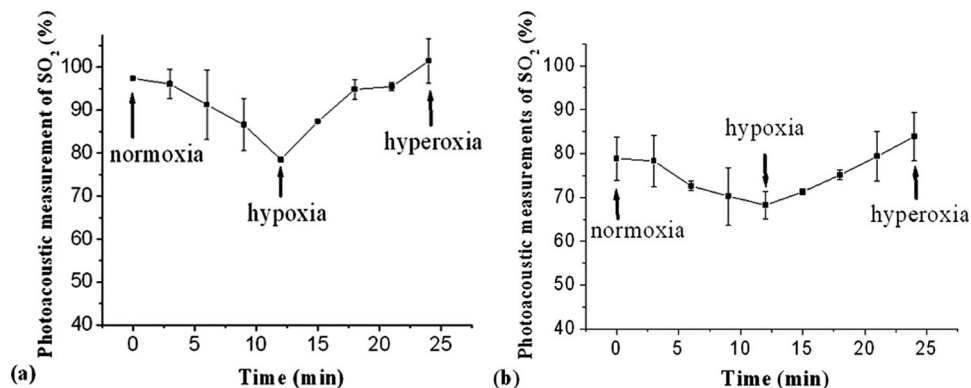


FIG. 5. Monitoring of changes in SO<sub>2</sub> in rabbit ear. (a) PA monitoring of SO<sub>2</sub> level changes in artery of rabbit ear from normoxia to hypoxia and to hyperoxia. (b) PA monitoring of SO<sub>2</sub> level changes in vein of rabbit ear from normoxia to hypoxia and to hyperoxia.

to hyperoxia gas and the arterial blood oxygenation of the rabbit increased to  $\sim 99\%$ . In this process, we acquired signals of the rabbit ear artery and vein, respectively, at three wavelengths. Each value of SO<sub>2</sub> involves three distinct PA signals at three wavelengths, which take about 40 s to acquire. Each value actually reflects a time-averaged quantity of the oxygen saturation. The functional changes in SO<sub>2</sub>, as a result of the physiological modulations, can be monitored by this system. Curve of blood oxygen saturation changes was presented by calculating the signals, which are obtained at an interval of 3 min. As shown in Fig. 4, from normoxia to hypoxia and to hyperoxia, continuous changes in SO<sub>2</sub> in vessels were monitored by PA technique. The SO<sub>2</sub> level of artery changed consistently from 97.4% to 79.5% and to 101.4%. The changes in SO<sub>2</sub> were  $\sim 18\%$  and  $\sim 22\%$  as a result of the inhaled gas that changed from normal to hypoxia and to hyperoxia, respectively [Fig. 5(a)]. Their veins were consistent from 78.9% to 68.2% and 83.92% [Fig. 5(b)]. The result in this work agrees with the physiology. There were standard deviations in the results due to the influence of different optical parameters in tissues at different wavelengths. In addition, the fluctuation of laser, which includes energy and skeleton, is another impact of accurate measurement of SO<sub>2</sub>. The experimental results show that our PA system has the capability to reflect the change in SO<sub>2</sub>.

#### IV. CONCLUSION

In this work, a multiwavelength PA system with double-ring sensor is demonstrated for noninvasive monitoring of oxygen saturation *in vivo*. Because the sensor has a good ultrasonic focusing effect, this multiwavelength PA system has a good lateral resolution, which is much better than pulse oximetry with no lateral resolution and can assess functional parameters and changes in localized vessels. Also this PA system could noninvasively monitor SO<sub>2</sub> in single subcutaneous vessels including arteries and veins. The precision of this system is proved through phantom and *in vitro* tests. SO<sub>2</sub> of rabbit is also measured instantly and verified in *in vivo* study. Similarly, the SO<sub>2</sub> detection in tissues is the same as that in blood vessels. This PA system can potentially be used for noninvasive, continuous real-time monitoring of the jugular venous oxygen saturation in therapy of head injury and digging skull operation.

In further study of monitoring of SO<sub>2</sub> *in vivo*, the distribution of optical energy in the tissue must be studied. In other words, those optical parameters such as the absorption, scattering, and refractive index of the skin, fats, and other tissues induced by the effects of different wavelengths should be calculated. The photon transport model will be used in our farther study for accurate measurement of SO<sub>2</sub>. Predicatively, the sensor combined with a fiber will become a hybridized PA detector, which is used for contacted measurement of SO<sub>2</sub> in clinics. Also a wide bandwidth sensor can monitor SO<sub>2</sub> of smaller vessels in tissues with higher spatial resolution.

#### ACKNOWLEDGMENTS

This research is supported by the Program for Changjiang Scholars and Innovative Research Team in University (Grant No. IRT0829), the National Natural Science Foundation of China (Grant Nos. 30627003 and 30870676), and the Natural Science Foundation of Guangdong Province (Grant No. 7117865).

- <sup>1</sup>M. Sheinberg, M. J. Kanter, C. S. Robertson, C. F. Contant, R. K. Narayan, and R. G. Grossman, *J. Neurosurg.* **76**, 212 (1992).
- <sup>2</sup>T. Nakajima, H. Ohsumi, and M. Kuro, *Anesth. Analg.* (Baltimore) **77**, 1111 (1993).
- <sup>3</sup>A. T. Minassian, N. Poirier, M. Pierrot, P. Menei, J. C. Granry, M. Ursino, and L. Beydon, *Anesthesiology* **91**, 985 (1999).
- <sup>4</sup>G. A. Millikan, *Rev. Sci. Instrum.* **13**, 434 (1942).
- <sup>5</sup>F. F. Jöbsis, *Science* **198**, 1264 (1977).
- <sup>6</sup>R. A. Kruger, K. K. Kopecky, A. M. Aisen, D. R. Reinecke, G. A. Kruger, W. L. Kiser, and J. D. Reinecke, *Radiology* **211**, 275 (1999).
- <sup>7</sup>Y. Zeng, D. Xing, Y. Wang, B. Yin, and Q. Chen, *Opt. Lett.* **29**, 1760 (2004).
- <sup>8</sup>L. Xiang, D. Xing, H. Gu, D. Yang, S. Yang, L. Zeng, and W. R. Chen, *J. Biomed. Opt.* **12**, 014001 (2007).
- <sup>9</sup>S. Yang, D. Xing, Y. Lao, D. Yang, L. Zeng, L. Xiang, and W. R. Chen, *Appl. Phys. Lett.* **90**, 243902 (2007).
- <sup>10</sup>S. Yang, D. Xing, Q. Zhou, L. Xiang, and Y. Lao, *Med. Phys.* **34**, 0094 (2007).
- <sup>11</sup>Z. Yuan and H. Jiang, *Appl. Phys. Lett.* **88**, 231101 (2006).
- <sup>12</sup>Q. Zhang, Z. Liu, P. R. Carney, Z. Yuan, H. Chen, S. N. Roper, and H. Jiang, *Phys. Med. Biol.* **53**, 1921 (2008).
- <sup>13</sup>P. C. Li, C. R. C. Wang, D. B. Shieh, C. W. Wei, C. K. Liao, C. Poe, S. Jhan, A. A. Ding, and Y. N. Wu, *Opt. Express* **16**, 18605 (2008).
- <sup>14</sup>P. C. Li, C. W. Wei, C. K. Liao, C. D. Chen, K. C. Pao, C. R. C. Wang, Y. N. Wu, and D. B. Shieh, *Proc. SPIE* **6086**, 60860M (2006).
- <sup>15</sup>R. V. Kuranov, V. V. Sapozhnikova, D. S. Prough, I. Cicenaitė, and R. O. Esenaliev, *Phys. Med. Biol.* **51**, 3885 (2006).

- <sup>16</sup>S. A. Ermilov, A. Conjusteau, K. Mehta, R. Lacewell, P. M. Henrichs, and A. A. Oraevsky, *Proc. SPIE* **6086**, 608609 (2006).
- <sup>17</sup>X. Wang, X. Xie, G. Ku, L. V. Wang, and G. Stoica, *J. Biomed. Opt.* **11**, 024015 (2006).
- <sup>18</sup>H. Zhang, K. Maslov, M. Sivaramakrishnan, G. Stoica, and L. V. Wang, *Appl. Phys. Lett.* **90**, 053901 (2007).
- <sup>19</sup>H. K. Park, D. Kim, and C. P. Grigoropoulos, *J. Appl. Phys.* **80**, 4072 (1996).
- <sup>20</sup>M. W. Sigrist, *J. Appl. Phys.* **60**, R83 (1986).
- <sup>21</sup>P. W. McCormick, M. Stewart, M. G. Goetting, and G. Balakrishnan, *Stroke* **22**, 596 (1991).
- <sup>22</sup>B. Chance, E. Borer, A. Evans, G. Holtom, J. Kent, M. Maris, K. Mccully, J. Northrop, and M. Shinkwin, *Ann. N.Y. Acad. Sci.* **551**, 1 (1988).
- <sup>23</sup>S. L. Jacques and S. A. Prahl, *Absorption Spectra for Biological Tissues* (Oregon Medical Laser Center, Oregon, 2004).
- <sup>24</sup>W. G. Zijlstra, A. Buursma, and O. W. van Assendelft, *Visible and Near Infrared Absorption Spectra of Human and Animal Hemoglobin, Determination and Application* (VSP, Amsterdam, 2000).
- <sup>25</sup>H. Wang, D. Xing, and L. Xiang, *J. Phys. D* **41**, 095111 (2008).
- <sup>26</sup>P. Scheid and M. Meyer, *J. Appl. Physiol.* **45**, 818 (1978).